https://doi.org/10.5194/egusphere-2023-2029
Preprint. Discussion started: 5 October 2023

Distribution, chemical and molecular composition of high and low-molecular-weight humic-like substances in ambient aerosols

Xingjun Fan[a,b,*], Ao Cheng[a], Xufang Yu[a], Tao Cao[b,c], Dan Chen[a], Wenchao Ji[a], Yongbing Cai[a], Fande Meng[a], Jianzhong Song[b,**], Ping'an Peng[b]

[a] College of Resource and Environment, Anhui Science and Technology University, Fengyang 233100, P. R. China

[b] State Key Laboratory of Organic Geochemistry, Guangzhou Institute of Geochemistry, Chinese Academy of Sciences, Guangzhou 510640, P. R. China

[c] University of Chinese Academy of Sciences, Beijing, 100049, PR China

* Corresponding authors

E-mail addresses: fanxj@ahstu.edu.cn (Xingjun Fan), songjzh@gig.ac.cn (Jianzhong Song)

https://doi.org/10.5194/egusphere-2023-2029
Preprint. Discussion started: 5 October 2023

Abstract

Humic-like Substances (HULIS) encompass a continuum of molecular weight (MW) ranges, yet our understanding of how HULIS characteristics vary with MW is still limited and not well-established. In this study, a combination of ultrafiltration and solid-phase extraction protocols was employed to fractionate the high MW (HMW, >1 kDa) and low MW (LMW, < 1kDa) HULIS fractions from ambient aerosols collected during summer and winter at a rural site. Subsequently, comprehensive characterization by using total organic carbon, high-performance size exclusion chromatography (HPSEC), UV-vis and fluorescence spectroscopy, Fourier-transform infrared spectroscopy (FTIR), negative electrospray ionization high resolution mass spectrometry (ESI- HRMS) were conducted. The results revealed that HMW HULIS were dominated by larger-sized chromophores, substantially constituting a higher fraction of total organic carbon and UV absorption at 254 nm than LMW HULIS. While both HMW and LMW HULIS shared similar fluorophore types and functional groups, the former exhibited higher levels of humification and a greater presence of polar functional groups (e.g., -COOH, >C=O). HRMS analysis further unveiled that molecular formulas within HMW HULIS generally featured smaller sizes but higher degrees of unsaturation and aromaticity compared to those within LMW HULIS fractions. This observation suggests the possibility of small molecules assembling to form the HMW HULIS through intermolecular weak forces. Moreover, HMW HULIS contained a higher proportion of CHON but fewer CHO compounds than LMW HULIS. In both HMW and LMW HULIS, the unique molecular formulas were primarily

https://doi.org/10.5194/egusphere-2023-2029
Preprint. Discussion started: 5 October 2023

characterized by lignin-like species, yet the former displayed a prevalence of N-enriched and highly aromatic species. Additionally, HMW HULIS contained more unique lipids-like compounds, while LMW HULIS exhibited a distinct presence of tannin-like compounds. These findings provide valuable insights into the distribution, optical properties, and molecular-level characteristics of HULIS in atmospheric aerosols, thereby advancing our understanding of their sources, composition, and environmental implications.

Keywords: Humic-Like Substances, molecular weight fractionation, optical properties, high-performance size exclusion chromatography, negative electrospray ionization-high resolution mass spectrometry

https://doi.org/10.5194/egusphere-2023-2029
Preprint. Discussion started: 5 October 2023

1. Introduction

HUmic-Like Substances (HULIS) are complex and heterogeneous mixtures of water-soluble organic matters (WSOM) that are of great importance in the atmospheric environment. They usually share similar physicochemical properties (e.g., acidity, absorption, fluorescence, functional groups) with naturally occurring humic substances (Graber and Rudich, 2006; Zheng et al., 2013) and are prevalent in fog, clouds, rainwater and ambient aerosols (Birdwell and Valsaraj, 2010; Fan et al., 2016a; Santos et al., 2012). With substantial hygroscopic and surface-active properties, HULIS enhance the hygroscopic growth of particles, thereby contributing to the formation of the cloud condensation nuclei and ice nuclei (Chen et al., 2021a; Dinar et al., 2007). Moreover, acting as an important component of brown carbon (BrC), HULIS effectively absorb near-ultraviolet and visible light, thus influencing the global radiative balance and atmospheric chemistry processes (Bao et al., 2022; Zhang et al., 2020). Furthermore, HULIS have the potential to catalyze the formation of reactive oxygen species, leading to potential adverse health effects (Ma et al., 2019; Zhang et al., 2022b).

The chemical composition of atmospheric HULIS exhibit significant heterogeneity and typically comprises macromolecular compounds containing aromatic rings with highly conjugated structures, as well as long-chain hydrocarbon with polar groups (e.g., -OH, -COOH, -NO2) (Fan et al., 2013; Huo et al., 2021). To unravel the structural characteristics and properties of HULIS, a range of analytical techniques, including absorption and fluorescence spectroscopy, Fourier transform infrared spectroscopy (FTIR), nuclear magnetic resonance spectroscopy (^{1}H NMR), have been

https://doi.org/10.5194/egusphere-2023-2029
Preprint. Discussion started: 5 October 2023

utilized (Huo et al., 2021; Qin et al., 2022; Zou et al., 2020). These studies have provided insights into the overall structural characteristics of complex HULIS, including their abundances, chemical and optical characteristics (Huo et al., 2021; Mukherjee et al., 2020; Win et al., 2018; Zhang et al., 2022b; Zheng et al., 2013). In recent years, high-resolution mass spectrometry (HRMS) techniques, such as Fourier transform ion cyclotron resonance mass spectrometry (FT-ICR-MS) and orbitrap HRMS, in combination with electrospray ionization (ESI), have emerged as powerful tools for elucidating the molecular-level characteristics of HULIS (Lin et al., 2012; Sun et al., 2021; Wang et al., 2019; Zou et al., 2023). By utilizing HRMS, researchers have gained deeper insights into the complexity and chemical heterogeneity of HULIS at the molecular level.

Operationally, HULIS are defined as the hydrophobic fraction of water-soluble organic matter (WSOM) typically extracted through solid-phase extraction (SPE) protocol (Fan et al., 2012; Zou et al., 2020). Thus, the abundance and characteristics of HULIS are contingent upon the chemical composition of WSOM. Previous studies have shown that aerosol WSOM, also known as brown carbon (BrC), are comprised of a continuum of molecular weight (MW) species, as revealed by high-performance exclusion chromatography (HPSEC) analysis (Di Lorenzo et al., 2017; Fan et al., 2023; Wong et al., 2019). These studies have highlighted that BrC typically consist of both high-MW (HMW) and low-MW (LMW) chromophores in various aerosols. For example, BrC emitted from fresh biomass burning (BB) are dominated by low MW chromophores (Di Lorenzo et al., 2017; Wong et al., 2019). However, BrC derived from

https://doi.org/10.5194/egusphere-2023-2029
Preprint. Discussion started: 5 October 2023

aged BB aerosols and ambient aerosols tend to possess more HMW chromophores that are highly chemically resistant (Di Lorenzo et al., 2017; Fan et al., 2023; Wong et al., 2019). Further characterizations of different MW BrC can be conducted using an ultrafiltration (UF) protocol (Fan et al., 2021). This approach enabled researchers to obtain the distributions of content, chromophores and fluorophores within various MW BrC fractions. Despite these advancements, the chemical structures and molecular composition of different MW HULIS fractions remain poorly understood. Consequently, a combination of UF and SPE protocols for the fractionation and characterization of MW-separated HULIS is crucial, as it not only provides insights into MW distributions but also illuminates the chemical heterogeneities of aerosols HULIS.

In this study, a combination of UF-SPE isolation protocol was developed to fractionate and characterize the MW HULIS fractions. Two distinct sets of ambient $PM_{2.5}$ samples collected during summer and winter periods were utilized to facilitate a comparative analysis of MW HULIS. Initially, the WSOM were fractionated into high-MW (HMW, >1 kDa) and low-LMW (LMW, <1 kDa) species using the UF protocol. Subsequently, the resulting MW MSOM fractions underwent SPE to obtain different MW HULIS fractions. The obtained HMW and LMW HULIS fractions were comprehensively characterized using advanced analytical techniques, including total organic carbon analysis, UV-vis and fluorescence spectroscopy, HPSEC, and HRMS to unveil their abundances, absorption and fluorescence properties, and molecular characteristics. The findings of this study hold great significance in advancing our understanding of the definition and molecular profiles of HULIS, as well as facilitating

https://doi.org/10.5194/egusphere-2023-2029
Preprint. Discussion started: 5 October 2023

further investigations into their potential impacts on the atmospheric environment.

2. Materials and methods

2.1. Atmospheric fine particles sampling

Atmospheric $PM_{2.5}$ were sampled on the rooftop of a building within the campus of Anhui Science and Technology University (32.21°N, 118.72°E), around 20 m above ground level. Detailed information regarding the sampling site can be found in our previous studies (Cao et al., 2022; Fan et al., 2021). The $PM_{2.5}$ samples were collected using a high-volume $PM_{2.5}$ sampler (JCH-1000, Juchuang Ltd., Qingdao) onto prebaked quartz fiber filters (8 × 10 inches, Whatman). Sampling took place from July 25 to August 12, 2021, during summer, and from December 19, 2021 to January 6, 2022, during winter. Blank filters were also collected as control samples. All aerosol $PM_{2.5}$ filter samples were stored at -20 °C in a freezer prior to analysis. The atmospheric pollutant data (NO_2, SO_2 and O_3) near sampling site during sampling period were obtained from the website (https://www.aqistudy.cn) and are summarized in Table S1. Additionally, the fire spots were investigated using data from the website (https://firms.modaps.eosdis.nasa.gov/map/) and are visualized in Fig. S1.

2.2. Application of UF-SPE for isolating MW HULIS fractions

Punches of summer and winter aerosol $PM_{2.5}$ filter samples were taken and combined for the extraction of water-soluble organic matter (WSOM), respectively. The filters were immersed in 300 mL of ultrapure water and subjected to ultrasonication for

https://doi.org/10.5194/egusphere-2023-2029
Preprint. Discussion started: 5 October 2023

30 min. The resulting suspensions were then filtered through a 0.22 μm membrane (Φ 47 mm, Jinteng, China) to obtain bulk WSOM samples. These bulk filtrates were further subjected to UF and SPE in tandem to obtain different MW HULIS fractions. Please refer to Fig. S2 for a schematic representation of the fractionation steps.

Before UF, the bulk WSOM were diluted to DOC concentration below 30 mg/L to minimize the concentration effects and prevent the accumulation of organic matters at the membrane surface during UF. The detailed UF procedure followed the profile described in our previous study (Fan et al., 2021). Briefly, each bulk WSOM solution was passed through a pre-cleaned 1 kDa cut-off membrane in a stirred UF cell (Amicon 8200, Millipore, USA), with a pressure at 0.2 MPa applied by ultrapure N_2. The concentration factor was ~10. The resulting retentate was considered as HMW (>1 kDa) WSOM, while the permeate solutions represented the LMW (<1 kDa) WSOM. Finally, each MW fraction was diluted to the initial volume for further treatment and analysis. Mass balances of WSOM during one-step UF process generally ranged from 92% to 99%, as determined by total organic carbon (TOC) and UV absorption at 254 nm (UV_{254}), indicating good performance of UF without substantial loss or organic contamination.

Subsequently, SPE was applied to isolate the so-called HULIS fractions from the bulk and each MW fraction of WSOM, following the protocol proposed in our previous studies (Fan et al., 2013; Zou et al., 2020). Briefly, the acidified aqueous samples were passed through pre-activated HLB columns (Waters Oasis, 500 mg/6 mL, USA). The fractions retained on the resins (referred to as HULIS) were eluted with pure methanol

https://doi.org/10.5194/egusphere-2023-2029
Preprint. Discussion started: 5 October 2023

and dried using a gentle stream of pure N_2. Finally, the bulk, HMW and LMW HULIS fractions were obtained. A blank filter control was performed using the same procedure described above, and the analysis signals of samples were corrected by blank control.

2.3. HPSEC analysis

The apparent MW distributions of MW HULIS fractions were analyzed using a high-performance liquid chromatography (HPLC) system (LC-20AT, Shimadzu, Japan) equipped with a refractive index detector (RID-10A, Shimadzu) and a diode array detector (SPD-M20A, Shimadzu). The wavelength of the diode array detector was set at 254 nm. Separation was performed using an aqueous gel filtration column (Polysep-GFC-P 3000, Phenomenex) preceded by a guard column (Polysep-GFC-P, Phenomenex). The mobile phase consisted of a mixture of water and methanol (90:10 v/v) containing 25 mM ammonium acetate (Di Lorenzo et al., 2017; Wong et al., 2019). The sample injection volume was 100 μL, and the flow rate was maintained at 1 mL min^{-1}. The HPSEC calibration was performed using a series of polyethylene glycol (PEG) standards (Kawasaki et al., 2011; Zhang et al., 2022c). The chromatographic peak areas were integrated to represent the abundances of corresponding MW species. It should be noted that the MW values estimated here are nominal rather than absolute.

The weight-average MW (Mw), number-average MW (Mn) and polydispersivity (ρ), were determined using the following equations (Song et al., 2010):

$$Mw=\frac{\sum_{i=1}^{n}(h_i MW_i)}{\sum_{i=1}^{n}h_i} \quad (1)$$

$$Mn=\frac{\sum_{i=1}^{n}h_i}{\sum_{i=1}^{n}(h_i/MW_i)} \quad (2)$$

https://doi.org/10.5194/egusphere-2023-2029
Preprint. Discussion started: 5 October 2023

$$\rho = \frac{Mw}{Mn} \quad (3)$$

where h_i and MW_i are the absorption intensity of the chromatogram and the MW of molecules corresponding to the *i*th retention time, respectively.

2.4. Measurements of WSOC content and optical properties

The concentration of water-soluble organic carbon (WSOC) in HMW and LMW HULIS was measured using a Shimadzu TOC analyzer (TOC-VCPN, Japan) following the non-purgeable organic carbon protocol.

The UV-vis spectra were recorded using a UV-vis spectrophotometer (UV 2600, Shimadzu, Japan) over a wavelength range of 200-700 nm with 1 nm increments. Excitation-emission matrix (EEM) spectra were determined using a fluorescence spectrophotometer (F4600, Hitachi, Japan). The scanning ranges for excitation (Ex) and emission (Em) wavelengths were 200-400 and 290-520 nm, respectively, with a scanning speed was 12,000 nm/min.

To characterize the chemical and optical properties of MW HULIS fractions, several commonly used spectra parameters were calculated, including the specific UV absorbance at 254 nm ($SUVA_{254}$), the UV absorbance ratio between 250 and 365 nm (E_2/E_3), spectra slope ratios (S_R), the absorption Angstrom exponent (AAE), and mass absorption efficiency (MAE_{365}), fluorescence indices (FI), biological index (BIX), and humification degree (HIX) (Fan et al., 2021; Li et al., 2022; Wu et al., 2021). Further details can be found in Text S1 of the Supporting Information (SI).

https://doi.org/10.5194/egusphere-2023-2029
Preprint. Discussion started: 5 October 2023

2.5. FTIR spectrometry

The functional groups in HMW and LMW HULIS were characterized using a Nicolet iS50 FTIR spectrometer (Thermal Fisher, USA). Before analysis, the freeze-dried MW HULIS and pure KBr were thoroughly mixed, finely ground, and pressed into pellets under dry conditions. Then, the FTIR spectra of samples were recorded within the wavenumbers ranging from 4000 to 400 cm^{-1}, with a resolution of 4 cm^{-1}. To ensure accuracy, each spectrum was baseline-corrected using the pure KBr spectrum.

2.6. HRMS analysis and data processing

The MW HULIS fractions were analyzed using a Q-Exactive mass spectrometer (Thermo Scientific, Germany) equipped with a heated electrospray ionization (ESI) source. The system operated in negative ESI mode with a resolution of 140,000 at m/z = 200. The detection mass range was set from 60 to 900 m/z. To ensure accurate mass measurements, mass calibration was carried out using a commercial standard mixture of ESI-L Low Concentration Tuning Mix (G1969-85000, Agilent, USA).

The acquired mass spectra were processed using Xcalibur software (V2.2, Thermo Scientific). The mathematically possible formulas for all ions were calculated with a signal-to-noise ratio (s/n) ≥ 5 using a mass tolerance of 5 ppm. The assigned molecular formulas followed specific constraints, with limitations on the following elements: C ≤ 50, H ≤ 100, O ≤ 20, N ≤ 3, S ≤ 2. Additionally, the elemental ratios of H/C, O/C, N/C, and S/C were constrained to the ranges of 0.3–3.0, 0–3.0, 0–0.5, and 0–2.0, respectively. The double-bond equivalents (DBE) and modified aromaticity index

https://doi.org/10.5194/egusphere-2023-2029
Preprint. Discussion started: 5 October 2023

(AI_{mod}) values of the assigned neutral assigned formula ($C_cH_hO_oN_nS_s$) were calculated using the equations (4-5) (He et al., 2023; Song et al., 2022):

$$\mathrm{DBE} = 1 + \frac{1}{2}(2c - h + n) \quad (4)$$

$$\mathrm{AI}_{mod} = \frac{1 + c - 0.5o - 0.5n - 0.5h}{c - 0.5o - n} \quad (5)$$

The intensity-weighted molecular parameters (X_w) of MW, H/C, O/C, DBE, and AI values were calculated according to the equation (6) (He et al., 2023; Zhang et al., 2021; Zou et al., 2023):

$$X_W = \frac{\sum(I_i \cdot X_i)}{\sum I_i} \quad (6)$$

where X represents the aforementioned parameters, and I_i denote the intensity for each assigned formula i.

3. Results and discussion

3.1. Size and distribution of MW HULIS fractions

3.1.1. Molecular size of HMW and LMW HULIS

Fig. 1 shows the HPSEC chromatograms of MW HULIS. Both HMW and LMW HULIS exhibit MW continuum distributions ranging from 100 to 20,000 Da, which is consistent with the reported distributions of BrC in BB-derived and various ambient aerosol in previous studies (Di Lorenzo et al., 2017; Fan et al., 2023; Wong et al., 2017). However, the chromatographic patterns for HMW HULIS clearly differ from those observed for LMW HULIS in both aerosol samples. As seen in Fig. 1, HMW HULIS display an additional and stronger absorption peak at around 4000 Da (peak *iii*), along with a more pronounced peak at 2200 Da (peak *ii*) and a similar magnitude peak at 570

https://doi.org/10.5194/egusphere-2023-2029
Preprint. Discussion started: 5 October 2023

Da (peak *i*) compared to LMW HULIS. This suggests that HMW HULIS contain the majority of larger molecular size chromophores within the bulk WSOM.

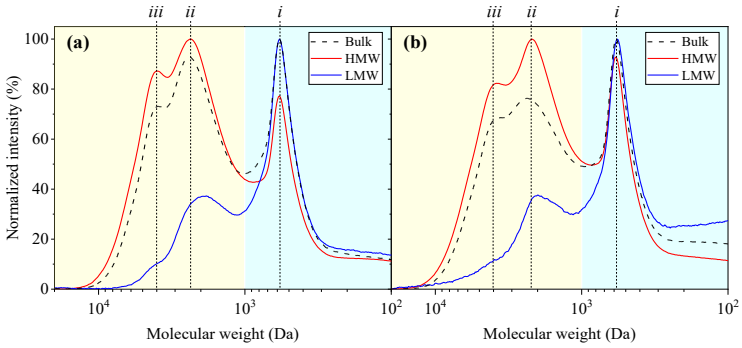

Fig. 1. Average HPSEC chromatograms of bulk, HMW and LMW HULIS fractions in (a) summer and (b) winter aerosol, respectively. The yellow and cyan shadows represent MW size regions of >1 kDa and <1 kDa, respectively.

Moreover, the molecular size of MW HULIS can be further reflected by the differences in Mw and Mn. As listed in Table 1, the average Mw and Mn of HMW HULIS are 2233-2315 and 654-707 Da, respectively, greatly lager than that of LMW HULIS (989-1071 and 293-394 Da, respectively). These differences indicate that the sources and formation processes of HMW HULIS may differ from LMW HULIS. Many previous studies have demonstrated that complex atmospheric aging processes significantly enhance the formation of large molecular size chromophores, while concurrently leading to the bleaching of small size ones (Di Lorenzo et al., 2018; Di Lorenzo et al., 2017; Wong et al., 2017; Wong et al., 2019). Therefore, the higher proportions of large-size chromophores and resulting larger apparent molecular size of HMW HULIS may indicate their possible secondary formation nature.

https://doi.org/10.5194/egusphere-2023-2029
Preprint. Discussion started: 5 October 2023

Table 1. The summary of typical quantity and quality parameters of each MW HULIS fraction from BB and ambient aerosols.

		Summer			Winter		
		Bulk	HMW	LMW	Bulk	HMW	LMW
HPSEC-derived parameters	Mw	1975±13	2315±38	1071±24	1918±56	2233±42	989±67
	Mn	591±53	707±48	394±13	525±57	654±17	293±32
	ρ	3.4±0.3	3.3±0.2	2.7±0.2	3.7±0.3	3.4±0.2	3.4±0.2
HULIS/WSOM (%)[a]	TOC	65±1	68±1	51±2	63±2	67±2	41±1
	UV_{254}	66±5	65±2	55±4	67±1	65±1	61±2
Optical parameters	E_2/E_3	12.02±0.54	11.72±0.31	14.98±0.98	6.30±0.24	6.54±0.16	7.24±0.43
	MAE_{365}	0.21±0.02	0.23±0.01	0.20±0.01	1.04±0.02	1.06±0.01	0.88±0.00
	AAE	7.11±0.32	7.59±0.00	8.25±0.23	6.66±0.06	6.25±0.06	7.28±0.03
	FI	2.00±0.04	1.99±0.03	2.04±0.05	2.06±0.01	1.97±0.03	2.25±0.02
	BIX	0.95±0.01	0.86±0.07	1.02±0.01	0.96±0.01	0.81±0.01	1.07±0.02
	HIX	2.42±0.06	2.43±0.04	2.40±0.05	3.13±0.25	5.64±0.34	1.94±0.16

[a] The ratios of contents of SPE-isolated HULIS fractions to that of corresponding WSOM fractions determined by TOC and/or absorbance at 254 nm (UV_{254}).

3.1.2. Relative abundances of HMW and LMW HULIS

The contribution of MW-HULIS fractions to their corresponding MW-WSOM fractions, quantified in terms of TOC and UV absorption at 254 nm for both summer and winter aerosols are summarized in Table 1. In general, the ratios of HULIS/WSOM of HMW fractions (in terms of TOC and UV254) (65-68%) were higher than the ratios (41-61%) observed for LMW fractions. This finding suggests that the higher presence of hydrophobic and conjugated aromatic structures in HMW WSOM, but more hydrophilic OC and non-aromatic species (e.g., aliphatic dicarboxylic acid) in the LMW WSOM (Fan et al., 2012; Zou et al., 2020).

Fig. 2 illustrates the distribution of distinct MW fractions within reconstructed

https://doi.org/10.5194/egusphere-2023-2029
Preprint. Discussion started: 5 October 2023

WSOM, wherein "non-HULIS" refers to the content differences between the MW WSOM and its HULIS fractions. The HMW HULIS fraction contributed 39-41% of TOC and 40-47% of UV254 to the bulk WSOM. In contrast, the LWM HULIS fraction only make up a smaller proportion, accounting for 16-20% of TOC and 17-21% of UV254 within the bulk WSOM. Specifically, the ratios between HMW HULIS and LMW HULIS (H/L) ranged from 1.88 to 2.75 for both summer and winter aerosols in terms of either TOC or UV254. These findings emphasize that HMW HULIS significantly dominate the bulk aerosol HULIS fractions. Notably, the H/L ratio for winter aerosols was higher than that for summer aerosols, suggesting that larger-sized HULIS contributed more to the bulk HULIS fractions in winter aerosols.

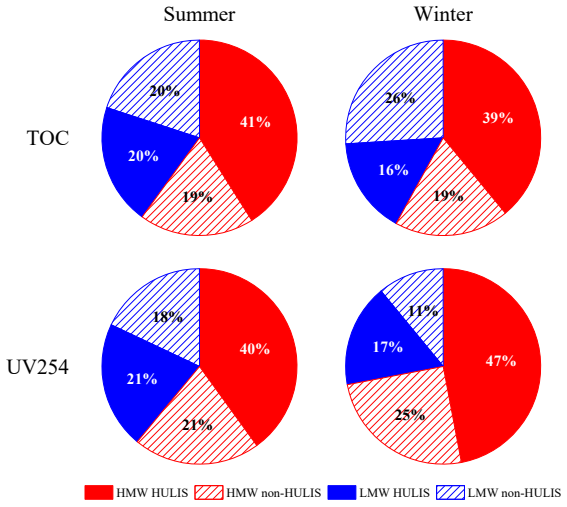

Fig. 2. Relative proportions of different MW fractions in summer and winter aerosols determined by TOC and UV254.

The non-HULIS fractions are also important constituents within aerosol WSOM, but exhibit some differences between HMW and LMW fractions. The contributions of

https://doi.org/10.5194/egusphere-2023-2029
Preprint. Discussion started: 5 October 2023

HMW non-HULIS to bulk WSOM were ~19% as determined by TOC and 21-25% measured by UV254. In case of LMW non-HULIS, the contributions were higher in terms of TOC (20-26%) but lower in terms of UV254 (11-18%). These results indicate that the LMW WSOM contain a larger proportion of hydrophilic organic species with weak or no light absorption.

3.2. Optical characteristics of MW HULIS fractions

3.2.1. Light absorption characteristics

The absorption spectra of MW HULIS fractions in ambient aerosols are shown in Fig. S3. These spectra exhibit a featureless shape with a general decrease in absorbance as the wavelength increases, which is a typical characteristic of HULIS found in rainwater, biomass burning (BB), and ambient aerosols (Huo et al., 2021; Santos et al., 2009; Zhang et al., 2022b). The E2/E3 ratio, commonly used as an indicator of the chemical characteristics of organic species, is inversely correlated with higher aromaticity and larger molecular weight (Fan et al., 2021; Li et al., 2022; Sun et al., 2021). As listed in Table 1, the E_2/E_3 of HMW HULIS fractions generally were lower than that of LMW HULIS in both ambient aerosols. This is consistent with the expectation that larger-sized HULIS generally possess more polyconjugated and polymeric structures (Fan et al., 2021; Zhang et al., 2022c), leading to greater aromaticity and larger molecular size.

MAE_{365} and AAE are commonly used to characterize the light absorption capacity and the spectral dependence of light absorption by aerosol chromophores, respectively

https://doi.org/10.5194/egusphere-2023-2029
Preprint. Discussion started: 5 October 2023

(Bao et al., 2022; Fan et al., 2016b; Kumar et al., 2017; Yuan et al., 2021; Zou et al., 2020). As listed in Table 1, the average MAE_{365} values of HMW HULIS are 0.23 and 1.06 m^2 g^{-1} in summer and winter aerosol, respectively. These values are higher than the corresponding values of 0.20 and 0.88 m^2 g^{-1}, respectively, for LMW HULIS. In addition, HMW HULIS presented lower AAE values, being 7.59 and 6.25 in summer and winter aerosol, respectively, than the corresponding values of 8.25 and 7.28, respectively, for LMW HULIS (Table 1). As shown in Fig. S4, the LMW HULIS exhibit lower MAE_{365} and higher AAE values, falling within the left-upper range of the values previously reported for various ambient aerosol-derived and BB-derived HULIS (Bao et al., 2022; Fan et al., 2018; Fan et al., 2016b; Hong et al., 2022; Huo et al., 2018; Liu et al., 2018; Ma et al., 2019; Sun et al., 2021; Tang et al., 2020; Wu et al., 2018; Wu et al., 2020; Yuan et al., 2021; Zhang et al., 2022a). It has been widely reported that pronounced photooxidation and photobleaching processes of BrC can lead to a reduction in their absorption capacity (Wu et al., 2018; Wu et al., 2020; Zhang et al., 2022a), but an enhancement of their spectra dependence on wavelength (Chen et al., 2021b; Sun et al., 2021). Therefore, it can be speculated that LMW HULIS are more susceptible to enrich the by-products resulting from the degradation and oxidation of BrC during processes like photooxidation and photobleaching.

3.2.2. Fluorescence characteristics

The EEM contours of MW HULIS fractions from both summer and winter aerosols are presented in Fig. S5. These HULIS fractions from both seasons exhibit

https://doi.org/10.5194/egusphere-2023-2029
Preprint. Discussion started: 5 October 2023

similar EEM spectra features, with a predominance of humic-like fluorophores (Ex/Em = 210-235/395-410 nm). This observation suggest that humic-like fluorophores are fundamental constituents of both HMW and LMW HULIS, which are consistent with previous findings for aerosols MW WSOM (Fan et al., 2021) and bulk HULIS in BB-derived and ambient aerosols (Fan et al., 2020; Qin et al., 2018). In this study, the fluorescence regional integration (FRI) method was applied to characterize the fluorescent composition of MW HULIS. Using FRI, EEM spectra were divided five fluorescence regions (labeled as I to V) (Fig. S5), which were successively assigned to simple aromatic proteins (I and II), fulvic acid-like (III), soluble microbial byproduct-like (IV), and humic acid-like (V) substances, respectively, as established in previous studies (Chen et al., 2003; Qin et al., 2018; Wang et al., 2021b). As shown in Fig. S6, the large-size aromatic proteins (II) and fulvic acid-like substances (III) dominated the fluorophores within MW HULIS in both summer and winter aerosols, comprising approximately 62-64% of the total fluorescence intensity. This finding is consistent with previous reports on bulk HULIS in summer and winter aerosols from industrial and urban cities (Qin et al., 2018; Wang et al., 2021b). In comparison, the HMW HULIS in both summer and winter aerosols generally exhibited a higher proportion of humic acid-like substances (V), while having a lower abundance of small-size aromatic proteins I compared to LMW HULIS. These differences are particularly pronounced in winter aerosols, with the humic acid-like substances accounting for 23% in HMW HULIS compared to 13% in LMW HULIS, and small-size aromatic proteins I comprising 9% in HMW HULIS compared to 17% in LMW HULIS (Fig. S6).

https://doi.org/10.5194/egusphere-2023-2029
Preprint. Discussion started: 5 October 2023

Furthermore, the higher HIX values of HMW HULIS (5.64) in comparison to LMW HULIS (1.94) further support these differences (Table 1). The pronounced BB emissions and potential NO_2-related oxidation of OA, as evidenced by the presence of more hotspots (Fig. S1) and higher concentration of NO_2 (Table S1), are likely driving these marked distinctions between HMW and LMW HULIS in winter aerosols. In general, these findings imply that the HMW HULIS have a stronger level of humification and oxidation, while the LMW HULIS appear to be of a simpler nature and are more likely associated with fresh emissions (e.g., BB).

3.2.3 Functional groups of MW HULIS

Fig. 3 depicts the FTIR spectra of HMW and LMW HULIS in both summer and winter aerosols. In general, both HMW and LMW HULIS present similar absorption peaks, including pronounced peaks at 3434 cm^{-1} (O-H stretching of phenols and carboxylic acids), 1721 cm^{-1} (mainly C=O stretching of carboxylic acids), 1636 cm^{-1} (mainly C=C stretching of aromatic rings and C=O stretching of conjugated carbonyl groups) and 1390 cm^{-1} (O-H deformation and C-O stretching of phenolic groups) were observed (Fan et al., 2020; Fan et al., 2016b; Mukherjee et al., 2020; Wang et al., 2021a). Additionally, weak peaks at 2929-2980 cm^{-1} and 1045-1281 cm^{-1}, attributed to C-H stretching of aliphatic $-CH_2$ and $-CH_3$, and C-O stretching of esters and ethers, respectively, were also observed (Fan et al., 2016b; Wang et al., 2021a; Zhang et al., 2021). These observations indicate that both HMW and LMW HULIS contain complex multi-component mixtures of compounds, encompassing aliphatic and aromatic species,

https://doi.org/10.5194/egusphere-2023-2029
Preprint. Discussion started: 5 October 2023

as well as carboxyl and phenolic functional groups.

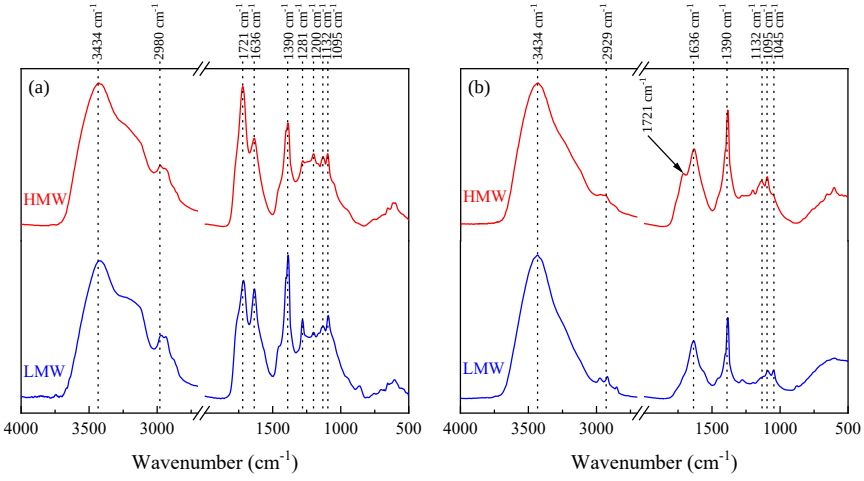

Fig. 3. FTIR spectra of HMW and LMW HULIS in (a) summer and (b) winter aerosols.

As shown in Fig. 3, more intense peaks at 1721 and 1636 cm^{-1} were observed in HULISs in summer aerosols compared to those in winter aerosols. In addition, the peaks at 1045-1281 cm^{-1} in summer HULISs appear to be more complex and overlapping than those in winter HULISs. These findings imply higher abundances of aromatic carboxyl acids and other O-containing groups (i.e., -OH, C=O and C-O) in summer HULISs than in winter ones, possibly attributed to complex oxidation reactions prevailing in summer season (Fan et al., 2020; Qin et al., 2022). This could be partly associated with the enhanced oxidation processes driven by the higher concentration of O_3 in summer (Table S1). Our previous study has proved that the O_3 oxidation of BB BrC lead to the generation of more intense peaks at approximately 1725 cm^{-1} (Fan et al., 2020). Moreover, distinct differences in relative peak intensity between HMW and LMW HULIS fractions were observed. HMW HULIS generally exhibit more intense at 1721

https://doi.org/10.5194/egusphere-2023-2029
Preprint. Discussion started: 5 October 2023

cm^{-1} compared to LMW HULIS in both seasonal aerosols (Fig. 3). This finding suggests that HMW HULIS contain a higher abundance of C=O groups, likely associated with the oxidation of the unsaturated structures with addition of polar functional groups (e.g., -COOH, >C=O) during SOA processes (Fan et al., 2020; Pillar-Little and Guzman, 2018).

3.3 Molecular-level insights into MW HULIS

3.3.1. Seasonal variations in the molecular composition of MW HULIS

The molecular-level characteristics of MW HULIS were examined using negative ESI- HR-MS analysis. Fig. 4 displays the reconstructed mass spectra of all HULIS fraction in both summer and winter aerosols. Hundreds of peaks can be observed in the spectra ranging from m/z 100 to 450 for all samples, with most ions being abundant within the m/z 150-350 range. These spectrum characteristics are similar to those previously reported for HULIS in ambient aerosols and BB emissions (He et al., 2023; Song et al., 2022; Sun et al., 2021; Wang et al., 2019; Zhang et al., 2021; Zou et al., 2023).

https://doi.org/10.5194/egusphere-2023-2029
Preprint. Discussion started: 5 October 2023

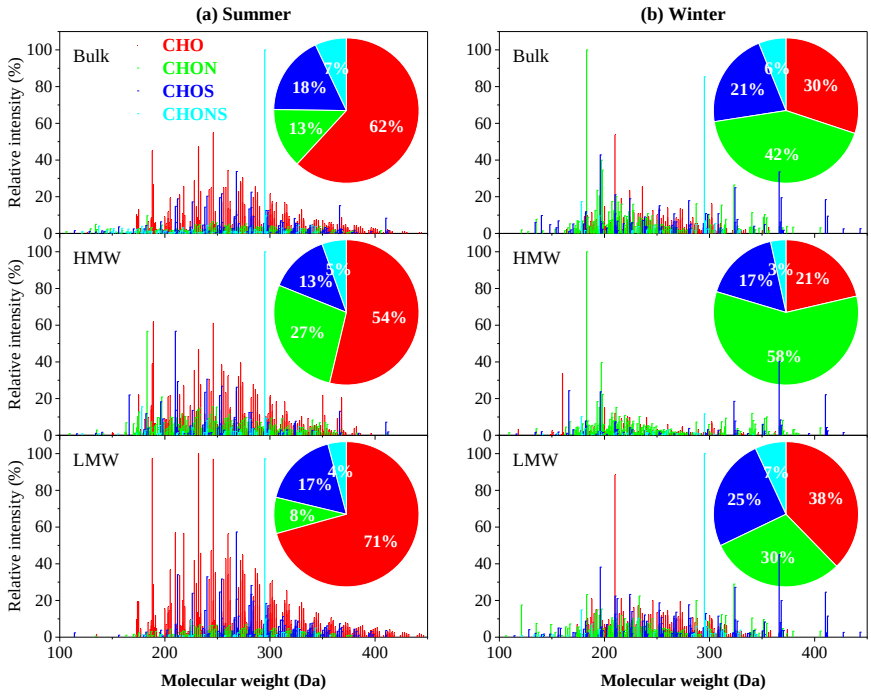

Fig. 4. Mass spectra of bulk and MW HULIS in (a) summer and (b) winter aerosols. The pie charts represent the intensity distributions of four compound categories (CHO, CHON, CHOS, and CHONS).

As listed in Table 2, the number of assigned formulas within MW HULIS in summer aerosols were 655-672, which was higher than the range of 470-506 observed in winter aerosols. This suggests that the MW HULIS in summer aerosols exhibited greater diversity than those in winter aerosols, mainly due to the stronger SOA formation that enhanced the heterogeneity of HULIS fractions in the summer. The identified formulas were then classified into four groups (i.e., CHO, CHON, CHOS and CHONS) according to their elemental composition. As depicted in pie charts in Fig. 4, summer HULISs are predominantly composed of CHO (54-71%), while winter

https://doi.org/10.5194/egusphere-2023-2029
Preprint. Discussion started: 5 October 2023

HULISs feature a high concentration of both CHON (30-58%) and CHO (21-38%). The notably higher content of CHO in summer HULISs are likely due to a wide distribution of biogenic VOC-derived SOAs during the summer season (Li et al., 2022; Sun et al., 2023). CHON content in winter HULISs is generally higher than in summer ones, potentially due to more significant contributions from direct BB, as well as secondary nitrogen-related chemical processes during the winter season (He et al., 2023; Song et al., 2022; Zhang et al., 2021; Zou et al., 2023). This finding is supported by the greater number of fire spots (Fig. S1) and higher concentrations of NO_2 (Table S1) during winter. The higher proportions of CHON compounds in aerosol HULIS typically lead to enhanced light absorption capabilities (He et al., 2023; Song et al., 2022; Zeng et al., 2021). This provides an strong explanation for why winter HULIS exhibit higher MAE_{365} values compared to summer HULIS. Additionally, CHOS is more abundant in winter HULISs (17-25%) than in summer aerosols (13-18%). Previous studies have demonstrated that both coal combustion and the oxidation initiated by SO_2 can lead to the generation of larger amounts of S-containing compounds (Song et al., 2018; Song et al., 2022; Zou et al., 2023). This finding suggested that the increased levels of coal combustion and SO_2-related SOAs, as evidenced by higher concentration of SO_2 (Table S1), are significant contributors to the presence of BrC in winter compared to in summer.

https://doi.org/10.5194/egusphere-2023-2029
Preprint. Discussion started: 5 October 2023

Table 2. The average values of intensity-weighted molecular weights (MW), elemental ratios, double bond equivalents (DBE), modified aromaticity index (AI_{mod}) and carbon oxidation state (OS_C) for tentatively identified compounds of the bulk and MW HULIS samples.

		Elemental compositions	Number of formulas	MW_w	H/C_w	O/C_w	N/C_w	S/C_w	O/N_w	O/S_w	OM/OC_w	DBE_w	DBE/C_w	$DBE\text{-}O_w$	$AI_{mod,w}$	$OS_{C,w}$
Summer	BULK	CHO	376	276	1.39	0.59					1.91	4.69	0.39	-2.20	0.15	-0.21
		CHON	270	260	1.35	0.60	0.15		5.52		2.10	4.99	0.50	-1.17	0.27	-0.14
		CHOS	133	278	1.74	0.71		0.11		6.61	2.38	2.21	0.24	-4.41	0.02	-0.33
		CHONS	81	265	1.69	0.59	0.18	0.14	4.98	5.20	2.49	3.38	0.36	-1.95	0.09	-0.52
		Total	860	273	1.47	0.61	0.03	0.03	1.09	1.54	2.06	4.20	0.38	-2.44	0.14	-0.24
	HMW	CHO	270	264	1.41	0.55					1.85	4.51	0.38	-1.70	0.16	-0.32
		CHON	264	248	1.42	0.61	0.14		5.23		2.09	4.44	0.47	-1.33	0.24	-0.20
		CHOS	72	247	1.82	0.75		0.14		5.83	2.53	1.81	0.22	-4.07	0.01	-0.32
		CHONS	39	269	1.55	0.64	0.19	0.15	4.87	5.16	2.60	3.82	0.44	-1.65	0.14	-0.28
		Total	645	258	1.48	0.60	0.05	0.03	1.70	1.07	2.05	4.09	0.39	-1.91	0.16	-0.29
	LMW	CHO	365	275	1.34	0.64					1.97	4.82	0.42	-2.47	0.16	-0.05
		CHON	155	272	1.39	0.66	0.11		6.60		2.12	4.80	0.45	-2.09	0.18	-0.08
		CHOS	120	284	1.71	0.74		0.11		7.05	2.43	2.51	0.25	-4.58	0.02	-0.22
		CHONS	32	322	1.71	0.64	0.11	0.11	6.59	6.63	2.42	3.32	0.30	-3.41	0.06	-0.42
		Total	672	278	1.42	0.66	0.01	0.02	0.80	1.48	2.08	4.36	0.39	-2.84	0.13	-0.10
Winter	BULK	CHO	142	247	1.23	0.48					1.75	5.35	0.47	-0.05	0.32	-0.26
		CHON	194	231	1.24	0.53	0.16		3.96		1.99	5.17	0.57	0.52	0.48	-0.18
		CHOS	79	271	1.93	0.51		0.11		4.97	2.14	1.21	0.14	-3.80	0.04	-0.91
		CHONS	20	271	1.61	0.69	0.16	0.13	5.60	5.90	2.60	3.32	0.40	-2.65	0.09	-0.24
		Total	435	247	1.41	0.52	0.08	0.03	2.02	1.42	1.99	4.27	0.44	-0.77	0.31	-0.37
	HMW	CHO	138	232	1.36	0.47					1.74	4.79	0.41	0.02	0.28	-0.42

https://doi.org/10.5194/egusphere-2023-2029
Preprint. Discussion started: 5 October 2023

	CHON	244	232	1.29	0.53	0.16		3.89		2.01	4.87	0.55	0.23	0.44	-0.23
	CHOS	59	292	2.08	0.40		0.12		4.40	2.04	0.46	0.06	-4.06	0.02	-1.27
	CHONS	29	236	1.74	0.48	0.22	0.20	2.82	3.02	2.57	2.88	0.38	-0.57	0.27	-0.77
	Total	470	242	1.46	0.50	0.10	0.03	2.37	0.85	1.98	4.04	0.43	-0.57	0.33	-0.46
LMW	CHO	176	249	1.23	0.54					1.82	5.25	0.48	-0.65	0.30	-0.15
	CHON	195	239	1.34	0.49	0.16		3.99		1.95	4.88	0.52	0.29	0.45	-0.36
	CHOS	107	280	1.94	0.54		0.10		5.42	2.17	1.20	0.13	-4.25	0.02	-0.85
	CHONS	28	272	1.67	0.69	0.16	0.14	5.89	6.03	2.63	2.99	0.37	-3.15	0.13	-0.29
	Total	506	256	1.47	0.54	0.06	0.04	1.61	1.78	2.01	3.96	0.39	-1.45	0.26	-0.40

https://doi.org/10.5194/egusphere-2023-2029
Preprint. Discussion started: 5 October 2023

Table 2 summarizes the intensity-weighted molecular parameters for MW HULIS in both summer and winter aerosols. Evidently, the MWw of summer HULISs are 258-278, which are higher than the corresponding values of 242-256 for winter HULISs. This observation indicates that summer HULISs exhibit larger sizes, consistent with their higher HPSEC-derived Mw and Mn compared to winter HULISs. Moreover, summer HULISs exhibit higher O/Cw ranging from 0.60 to 0.66, as well as $OS_{C,w}$ ranging from -0.29 to -0.10, which exceed the respective values of 0.50 to 0.54 and -0.46 to -0.37 observed in winter HULISs. Conversely, winter HULISs display higher $AI_{mod,w}$ values (0.26-0.33) than those (0.13-0.16) for summer ones. These findings suggest that summer HULISs are characterized by a high degree of oxidation, while winter HULISs exhibit stronger aromaticity.

3.3.2. Comparison on molecular composition of HMW and LMW HULIS

CHO compounds. The CHO compounds are prominent constituents within HULIS fractions, accounting for 54% and 21% in summer and winter HMW HULIS, respectively, whereas these proportions increase to 71% and 38% in LMW HULIS (Fig. 4). It is worth noting that CHO compounds that undergo deprotonation in ESI- mode are likely associated with the presence of carboxyl, carbonyl, alcohol and ester (Lin et al., 2012; Wang et al., 2018). Moreover, CHO compounds in LMW HULIS exhibit a higher oxygenation level compared to HMW HULIS, as evidenced by the higher O/C_w and $OS_{C,w}$ values. As shown in Table 2, the O/C_w for CHO in LMW HULIS are 0.55-0.64, which are higher than 0.47-0.54 observed in HMW HULIS. In contrast, the H/Cw

https://doi.org/10.5194/egusphere-2023-2029
Preprint. Discussion started: 5 October 2023

for CHO in HMW HULIS were consistently higher than those in LMW HULIS, with values of 1.41 vs. 1.34 in summer and 1.36 vs. 1.23 in winter (Table 2). This disparity strongly suggests a higher saturation level of CHO compounds within HMW HULIS. This conclusion is further corroborated by the lower DBE_w and $AI_{mod,w}$ observed for CHO in HMW HULIS compared to LMW HULIS (Table 2). It is known that these values serve as estimations of C=C density and aromatic and condensed aromatic structures (Song et al., 2022; Zhang et al., 2021). Taken together, the CHO compounds within HMW HULIS exhibit a more aliphatic nature but lower aromaticity and oxidation levels when compared to those within LMW HULIS.

CHON compounds. HMW HULIS fractions consist of a higher proportion of CHON compounds compared to LMW HULIS, with proportions of 27% vs. 8% in summer and 58% vs. 30% in winter (Fig. 4). This observation suggests that HMW HULIS contain a higher content of N-containing components. It is noted that the LMW HULIS are generally characterized by higher O/Nw values of 6.60 in summer and 3.99 in winter compared to 5.23 in summer and 3.89 in winter for HMW HULIS. This indicates that the CHON compounds within LMW HULIS are more highly oxidized than those within HMW HULIS. In general, compounds with O/N ≥ 3 are indicative of oxidized N groups such as nitro ($-NO_2$) or nitrooxy ($-ONO_2$), while compounds with O/N < 3 may denote the reduced N-containing functional groups (i.e., amines) (He et al., 2023; Song et al., 2022; Zeng et al., 2021). In this study, a majority of the CHON compounds, comprising 73-85% in summer and 59-64% in winter, exhibited O/N ≥ 3 in both MW HULIS fractions. This suggests that high concentrations of nitro

https://doi.org/10.5194/egusphere-2023-2029
Preprint. Discussion started: 5 October 2023

compounds or organonitrates dominate the CHON compounds (Sun et al., 2023; Wang et al., 2018; Zeng et al., 2021), especially in summer samples, primarily due to the hydroxyl radical oxidation of biogenic or anthropogenic VOC precursors, as well as BB emissions (Song et al., 2022; Sun et al., 2021; Zhang et al., 2021; Zou et al., 2023). Furthermore, the CHON compounds exhibiting O/N ≥ 3 were more abundant in LMW HULIS compared to HMW HULIS, accounting for 85% vs. 73% in summer and 64% vs. 59% in winter. In contrast, HMW HULIS contained more CHON compounds with O/N < 3 compared to LMW HULIS. These findings collectively indicate that the CHON within HMW HULIS possess lower content of nitro compounds or organonitrates than LMW HULIS. Based on FTIR analysis, it is known that HMW HULIS contain more carboxylic groups than LMW HULIS, which indicate a higher likelihood of HMW HULIS containing more amino acids.

CHOS and CHONS compounds. In this study, we observed that CHOS accounted for proportions of 13% to 25% in all MW HULIS fractions, while CHONS had a lower proportion of 3% to 7% (Fig. 4). Notably, the distribution of CHOS differed between HMW and LMW HULIS in both season samples. As depicted in Fig. 4, HMW HULIS contained fewer CHOS compounds compared to LMW HULIS, with proportions of 13% vs. 17% in summer and 17% vs. 25% in winter. This finding suggests that a greater number of CHOS compounds are incorporated into the LMW HULIS fractions, which potentially leading to a reduction in the light absorption of LMW HULIS (Zeng et al., 2021; Zhang et al., 2021). Furthermore, as indicated in Table 2, both the CHOS and CHONS within LMW HULIS exhibited higher O/Sw values than

https://doi.org/10.5194/egusphere-2023-2029
Preprint. Discussion started: 5 October 2023

HMW HULIS in both seasonal samples. Consequently, the S-containing compounds within LMW HULIS were characterized by a higher degree of oxidation, primarily attributed to SO_2-related chemical oxidation process, in comparison to those in HMW HULIS. Moreover, it was observed that 61% to 92% of CHOS compounds exhibited O/S > 4, and 3% to 43% of CHONS compounds with O/S > 7 for all MW HULIS fractions. Among them, HMW HULIS own lower proportions of CHOS with O/S > 4 and CHONS with O/S > 7 than LMW HULIS, suggesting a reduced presence of potential organosulfates and nitrooxyorganosulfates within HMW HULIS (Sun et al., 2023; Wang et al., 2018; Zeng et al., 2021; Zou et al., 2023).

3.3.3. Comparative analysis of unique molecular formulas in HMW and LMW HULIS

In this study, particular emphasis was placed on the unique molecular formulas within the HMW or LMW HULIS fractions. Fig. 5a, b illustrates the Van Krevelen (VK) diagram depicting the distribution of unique molecular formulas within HMW and LMW HULIS in summer and winter samples. It is evident that a majority of unique formulas within LMW HULIS are concentrated around the origin with O/C > 0.5, accounting for 83% in summer and 64% in winter. In contrast, most formulas within HMW HULIS exhibited O/C < 0.5, representing about 58% for both seasonal samples. These findings indicate that the unique molecules within LMW HULIS consist of more polar O-containing organic compounds than those within HMW HULIS.

https://doi.org/10.5194/egusphere-2023-2029
Preprint. Discussion started: 5 October 2023

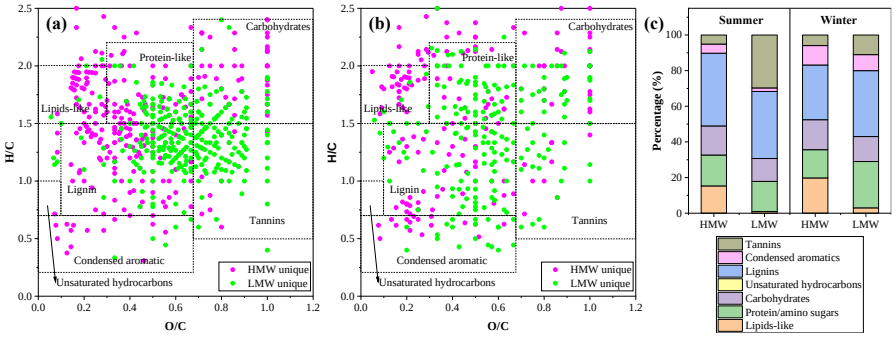

Fig. 5. Van Krevelen diagrams for the unique molecular formulas within HMW and LMW HULIS from (a) summer and (b) winter aerosols. (c) The contributions of major substances classes in unique formulas.

The molecular formulas are further categorized into seven groups based on previous studies, including lignin-like species, protein/amino sugars, condensed aromatics, tannin-like species, carbohydrate-like species, unsaturated hydrocarbons, and lipid-like species (He et al., 2023; Sun et al., 2021; Sun et al., 2023). The classification rules for these formulas can be found in Table S2. Fig. 5c provides an overview of the relative contributions of the number of unique formulas from each of the seven groups for HMW and LMW HULIS. The results indicate that the dominant substance class in the unique formulas within both MW HULIS are lignin-like species, accounting for proportions of 31-40%. This finding indicates that lignin derivatives are fundamental components in both HMW and LMW HULIS either in summer or winter aerosols. Additionally, there are notable differences in the molecular characteristics of lignin-like species within HMW and LMW HULIS. As listed in Table S3, lignin-like species within HMW HULIS exhibit lower MWw and O/Cw, but higher N/Cw and AImod,w values than those within LMW HULIS in both seasonal samples. These

https://doi.org/10.5194/egusphere-2023-2029
Preprint. Discussion started: 5 October 2023

observations suggest that the unique lignin-like substances in HMW HULIS likely contain more N-enriched and highly aromatic species, while those in LMW HULIS tend to concentrate more aliphatic O-containing compounds. These distinctions in composition and characteristics between HMW and LMW HULIS fractions provide valuable insights into their origins and transformations in the atmosphere.

Moreover, there are notable variations in the contributions of lipids-like, protein/amino sugars, carbohydrates, condensed aromatics, and tannins species between HMW and LMW HULIS. In general, HMW HULIS have a higher proportion of lipids-like species, carbohydrates and condensed aromatics than LMW HULIS in both summer and winter aerosols. Among these, the most remarkable difference in composition between HMW HULIS and LMW HULIS is seen in lipids-like species, accounting for 15% versus 1% in summer and 20% versus 3% in winter (Fig. 5). As reported in previous studies, lipids-like species primarily originate from biogenic emissions (He et al., 2023; Li et al., 2022; Sun et al., 2021). This suggests that there is a stronger contribution from biogenic emissions to HMW HULIS. Additionally, these species in HMW HULIS were usually characterized by lower DBE_w and slightly lower $OS_{C,w}$ when compared to LMW HULIS (Table S3), indicating they present stronger saturation and fewer oxidized substituents. On the other hand, tannins species contribute a higher proportion to LMW HULIS, constituting 30% in summer and 11% in winter, while comprising only 5%-6% in HMW HULIS in both season aerosols. Tannin-like species are known to consist of various polyphenolic groups containing hydroxyl and carboxylic functional groups (He et al., 2023; Li et al., 2022; Ning et al.,

https://doi.org/10.5194/egusphere-2023-2029
Preprint. Discussion started: 5 October 2023

2019; Sun et al., 2021). The slightly lower DBEw but much higher DBE-Ow for unique tannin-like species within HMW HULIS were observed compared to LMW HULIS (Table S3), suggesting that the former ones are enriched in more unsaturated O-containing functional groups, particularly carboxylic functional groups.

3.4. Atmospheric implications

This study provides comprehensive comparison between HMW and LMW HULIS regarding their distributions, chemical structures, molecular sizes and compositions. HMW HULIS appear to be larger than LMW HULIS, as evidenced by both ultrafiltration natures and the MW distributions of chromophores analyzed by HPSEC. However, HRMS analysis revealed that the average MWw of identified formulas within HMW HULIS were lower than those of LMW HULIS (Table 2). This discrepancy can likely be attributed to the "assembled structures" that construct the aerosol HULIS, as suggested in many previous studies focusing on HULIS and BrC characterization (Fan et al., 2021; Fan et al., 2023; Phillips et al., 2017; Qin et al., 2022). In fact, the results from EEM-FRI and FTIR analysis support the notion that HMW and LMW HULIS likely consist of potential structures assembled by similar basic fluorophores and functional groups. Based on this theory, HMW HULIS may consist of macromolecular species primarily assembled from small molecules through weak forces (i.e., π–π, van der Waals, hydrophobic, or hydrogen bonds) and/or charge-transfer interactions (Fan et al., 2021; Phillips et al., 2017), which can potentially disassemble during ESI ionization and form low MW molecules.

https://doi.org/10.5194/egusphere-2023-2029
Preprint. Discussion started: 5 October 2023

Based on the molecular-level characterization, significant distinctions in properties between HMW HULIS and LMW HULIS become evident. HMW HULIS generally exhibit stronger aromaticity but lower oxidation degree when compared to LMW HULIS. In terms of molecular composition, HMW HULIS contain higher quantities of CHON species but lower quantities of CHO compounds than LMW HULIS. Furthermore, more lipids-like species were identified as unique molecules in HMW HULIS, while more tannin-like species with abundant carboxylic groups were observed as unique molecules in LMW HULIS. Given these pronounced differences between HMW and LMW HULIS, it can be speculated that the higher levels of aromatic structures, greater presence of CHON molecules and the presence of lipids-like species may serve as driving factors in the formation of potential assembled structures in HMW HULIS. Additionally, it is well-established that CHON can enhance the light absorption of organic aerosols (OA), while CHO species may have the opposite effect, weakening light absorption (He et al., 2023; Song et al., 2022; Wang et al., 2019; Zeng et al., 2021). Therefore, it is reasonable to conclude that HMW HULIS possess stronger light absorbing capability, which is consistent with their larger MAE_{365} values.

Importantly, HMW HULIS contain amounts of carboxylic functional groups, reduced nitrogen species (e.g., amines) and aromatic species than LMW HULIS. These functional groups have strong complexation abilities with transition metals (Wang et al., 2021a; Wang et al., 2021b), thus influencing the transformation and chemical behavior of metals. Moreover, the OA-metals complex can potentially enhance the catalytic generation of reactive oxygen species (ROS) in organic aerosols (Win et al.,

https://doi.org/10.5194/egusphere-2023-2029
Preprint. Discussion started: 5 October 2023

2018; Zhang et al., 2022a), thereby playing significant roles in adverse health effects of OA. These results reinforce the significance of HMW HULIS in light absorption, metal complexation, and the potential ROS generation ability of aerosol BrC.

4. Conclusions

This study successfully isolated and characterized HMW and LMW HULIS in atmospheric aerosols using the UF-SPE technique, yielding insights into their distribution, optical properties and molecular-level characteristics. Both HMW and LMW HULIS exhibited a continuum of MW distributions ranging from 100 to 20,000 Da. However, HMW HULIS displayed more extensive and intricate MW distributions, suggesting differences in their sources and formation processes compared to LMW HULIS. In general, HMW HULIS constituted a higher percentage of TOC and UV254 in aerosols compared to LMW HULIS, indicating the prevalence of hydrophobic and conjugated aromatic structures in the former. Moreover, HMW HULIS exhibited higher aromaticity, stronger light absorption abilities, weaker spectra dependence, and stronger humification and conjugation, compared to LMW HULIS. Interestingly, HRMS analysis revealed slightly lower MWw values for HMW HULIS than LMW HULIS, which contradicted the HPSEC results and the nature of UF fractionation. This finding strongly suggests the possibility of small molecules assembling to form macromolecules in HMW HULIS. Regarding molecular composition, HMW HULIS contained a higer proportion of CHON compounds, constituting 27% vs. 8% in summer and 58% vs. 30% in winter, while LMW HULIS were primarily composed of CHO

https://doi.org/10.5194/egusphere-2023-2029
Preprint. Discussion started: 5 October 2023

compounds, accounting for 71% vs. 54%% in summer and 38% vs. 21% in winter. Both HMW and LMW HULIS featured lignin-like substances as major unique molecular formulas, but HMW HULIS exhibited more N-enriched and highly aromatic species, whereas LMW HULIS contained a higher proportion of polar O-containing functional groups. Additionally, HMW HULIS included a greater number of unique lipids-like compounds, while LMW HULIS tend to concentrate more tannin-like compounds. These observations shed light on the complex nature of MW HULIS, and their diverse sources and transformations. Future research should expand the geographical and seasonal coverage to gain a more comprehensive understanding of the molecular-level characteristics of MW HULIS in various atmospheric environments. Furthermore, exploring additional physicochemical properties of MW HULIS will provide valuable insights into their potential health and environmental implications. Overall, this study offers valuable insights into the molecular-level characteristics of aerosol HULIS, enhancing our understanding of their evolution, sources and potential environmental effects.

Author contribution

Xingjun Fan: Methodology, Supervision, Funding acquisition, Writing-review & editing. **Ao Cheng:** Sampling, Data curation. **Xufang Yu:** Writing-review & editing. **Tao Cao:** Sampling, Investigation. **Dan Chen:** Investigation, Data curation. **Wenchao Ji:** Formal analysis. **Yongbing Cai:** Writing-review & editing. **Fande Meng:** Writing-review & editing. **Jianzhong Song:** Methodology, Writing-review & editing. **Pingan Peng:** Writing-review & editing.

https://doi.org/10.5194/egusphere-2023-2029
Preprint. Discussion started: 5 October 2023

Declaration of Competing Interest

The authors declare that they have no known competing financial interests or personal relationships that could have appeared to influence the work reported in this paper.

Acknowledgments

This study was supported by the Natural Science Foundation of China (42192514, 52100114), the Anhui Provincial Natural Science Foundation (2108085MD140, 2108085QB56), and the State key Laboratory of Organic Geochemistry, GIGCAS (SKLOG202101), Anhui Provincial Key Science Foundation for Outstanding Young Talent (2022AH030145, gxyqZD2021126).

References

Bao, M., Zhang, Y.-L., Cao, F., Lin, Y.-C., Hong, Y., Fan, M., Zhang, Y., Yang, X., Xie, F., 2022. Light absorption and source apportionment of water soluble humic-like substances (HULIS) in PM2.5 at Nanjing, China. Environmental Research 206, 112554.

Birdwell, J.E., Valsaraj, K.T., 2010. Characterization of dissolved organic matter in fogwater by excitation–emission matrix fluorescence spectroscopy. Atmos. Environ. 44, 3246-3253.

Cao, T., Li, M., Xu, C., Song, J., Fan, X., Li, J., Jia, W., Peng, P., 2022. Technical note: Identification of chemical composition and source of fluorescent components in atmospheric water-soluble brown carbon by excitation-emission matrix with parallel factor analysis: Potential limitation and application. Atmos. Chem. Phys. Discuss. 2022, 1-41.

Chen, J., Wu, Z.J., Zhao, X., Wang, Y.J., Chen, J.C., Qiu, Y.T., Zong, T.M., Chen, H.X., Wang, B.B., Lin, P., Liu, W., Guo, S., Yao, M.S., Zeng, L.M., Wex, H., Liu, X., Hu, M., Li, S.M., 2021a. Atmospheric Humic-Like Substances (HULIS) Act as Ice Active Entities. Geophysical Research Letters 48, e2021GL092443.

Chen, Q., Hua, X., Dyussenova, A., 2021b. Evolution of the chromophore aerosols and its driving factors in summertime Xi'an, Northwest China. Chemosphere 281, 130838.

Chen, W., Westerhoff, P., Leenheer, J.A., Booksh, K., 2003. Fluorescence Excitation-Emission Matrix Regional Integration to Quantify Spectra for Dissolved Organic Matter. Environ. Sci. Technol. 37, 5701-5710.

Di Lorenzo, R.A., Place, B.K., VandenBoer, T.C., Young, C.J., 2018. Composition of Size-Resolved Aged Boreal Fire Aerosols: Brown Carbon, Biomass Burning Tracers, and Reduced Nitrogen. ACS Earth and Space Chemistry 2, 278-285.

Di Lorenzo, R.A., Washenfelder, R.A., Attwood, A.R., Guo, H., Xu, L., Ng, N.L., Weber, R.J., Baumann,

https://doi.org/10.5194/egusphere-2023-2029
Preprint. Discussion started: 5 October 2023

K., Edgerton, E., Young, C.J., 2017. Molecular-Size-Separated Brown Carbon Absorption for Biomass-Burning Aerosol at Multiple Field Sites. Environ. Sci. Technol. 51, 3128-3137.

Dinar, E., Taraniuk, I., Graber, E.R., Anttila, T., Mentel, T.F., Rudich, Y., 2007. Hygroscopic growth of atmospheric and model humic-like substances. J.Geophys. Res. 112.

Fan, X., Cai, F., Xu, C., Yu, X., Wang, Y., Xiao, X., Ji, W., Cao, T., Song, J., Peng, P.a., 2021. Molecular weight-dependent abundance, absorption, and fluorescence characteristics of water-soluble organic matter in atmospheric aerosols. Atmos. Environ. 247.

Fan, X., Cao, T., Yu, X., Wang, Y., Xiao, X., Li, F., Xie, Y., Ji, W., Song, J., Peng, P., 2020. The evolutionary behavior of chromophoric brown carbon during ozone aging of fine particles from biomass burning. Atmos. Chem. Phys. 20, 4593-4605.

Fan, X., Cheng, A., Chen, D., Cao, T., Ji, W., Song, J., Peng, P., 2023. Investigating the molecular weight distribution of atmospheric water-soluble brown carbon using high-performance size exclusion chromatography coupled with diode array and fluorescence detectors. Chemosphere 338, 139517.

Fan, X., Li, M., Cao, T., Cheng, C., Li, F., Xie, Y., Wei, S., Song, J., Peng, P.a., 2018. Optical properties and oxidative potential of water- and alkaline-soluble brown carbon in smoke particles emitted from laboratory simulated biomass burning. Atmos. Environ. 194, 48-57.

Fan, X., Song, J., Peng, P., 2013. Comparative study for separation of atmospheric humic-like substance (HULIS) by ENVI-18, HLB, XAD-8 and DEAE sorbents: elemental composition, FT-IR, 1H NMR and off-line thermochemolysis with tetramethylammonium hydroxide (TMAH). Chemosphere 93, 1710-1719.

Fan, X., Song, J., Peng, P.a., 2016a. Temporal variations of the abundance and optical properties of water soluble Humic-Like Substances (HULIS) in PM2.5 at Guangzhou, China. Atmos. Res. 172–173, 8-15.

Fan, X., Wei, S., Zhu, M., Song, J., Peng, P., 2016b. Comprehensive characterization of humic-like substances in smoke PM2.5 emitted from the combustion of biomass materials and fossil fuels. Atmos. Chem. Phys. 16, 13321-13340.

Fan, X.J., Song, J.Z., Peng, P.A., 2012. Comparison of isolation and quantification methods to measure humic-like substances (HULIS) in atmospheric particles. Atmos. Environ. 60, 366-374.

Graber, E.R., Rudich, Y., 2006. Atmospheric HULIS: How humic-like are they? A comprehensive and critical review. Atmos. Chem. Phys. 6, 729-753.

He, T., Wu, Y., Wang, D., Cai, J., Song, J., Yu, Z., Zeng, X., Peng, P.a., 2023. Molecular compositions and optical properties of water-soluble brown carbon during the autumn and winter in Guangzhou, China. Atmos. Environ. 296, 119573.

Hong, Y., Cao, F., Fan, M.-Y., Lin, Y.-C., Bao, M., Xue, Y., Wu, J., Yu, M., Wu, X., Zhang, Y.-L., 2022. Using machine learning to quantify sources of light-absorbing water-soluble humic-like substances (HULISws) in Northeast China. Atmos. Environ. 291, 119371.

Huo, Y., Li, M., Jiang, M., Qi, W., 2018. Light absorption properties of HULIS in primary particulate matter produced by crop straw combustion under different moisture contents and stacking modes. Atmos. Environ. 191, 490-499.

Huo, Y., Wang, Y., Qi, W., Jiang, M., Li, M., 2021. Comprehensive characterizations of HULIS in fresh and secondary emissions of crop straw burning. Atmos. Environ. 248, 118220.

Kawasaki, N., Matsushige, K., Komatsu, K., Kohzu, A., Nara, F.W., Ogishi, F., Yahata, M., Mikami, H., Goto, T., Imai, A., 2011. Fast and precise method for HPLC–size exclusion chromatography

https://doi.org/10.5194/egusphere-2023-2029
Preprint. Discussion started: 5 October 2023

with UV and TOC (NDIR) detection: Importance of multiple detectors to evaluate the characteristics of dissolved organic matter. Water Res. 45, 6240-6248.

Kumar, V., Goel, A., Rajput, P., 2017. Compositional and surface characterization of HULIS by UV-Vis, FTIR, NMR and XPS: Wintertime study in Northern India. Atmos. Environ. 164, 468-475.

Li, X., Yu, F., Cao, J., Fu, P., Hua, X., Chen, Q., Li, J., Guan, D., Tripathee, L., Chen, Q., Wang, Y., 2022. Chromophoric dissolved organic carbon cycle and its molecular compositions and optical properties in precipitation in the Guanzhong basin, China. Sci. Total Environ. 814, 152775.

Lin, P., Rincon, A.G., Kalberer, M., Yu, J.Z., 2012. Elemental composition of HULIS in the Pearl River Delta Region, China: results inferred from positive and negative electrospray high resolution mass spectrometric data. Environ. Sci. Technol. 46, 7454-7462.

Liu, J., Mo, Y., Ding, P., Li, J., Shen, C., Zhang, G., 2018. Dual carbon isotopes (14C and 13C) and optical properties of WSOC and HULIS-C during winter in Guangzhou, China. Sci. Total Environ. 633, 1571-1578.

Ma, Y., Cheng, Y., Qiu, X., Cao, G., Kuang, B., Yu, J.Z., Hu, D., 2019. Optical properties, source apportionment and redox activity of humic-like substances (HULIS) in airborne fine particulates in Hong Kong. Environmental Pollution 255, 113087.

Mukherjee, A., Dey, S., Rana, A., Jia, S., Banerjee, S., Sarkar, S., 2020. Sources and atmospheric processing of brown carbon and HULIS in the Indo-Gangetic Plain: Insights from compositional analysis. Environmental Pollution 267, 115440.

Ning, C., Gao, Y., Zhang, H., Yu, H., Wang, L., Geng, N., Cao, R., Chen, J., 2019. Molecular characterization of dissolved organic matters in winter atmospheric fine particulate matters (PM2.5) from a coastal city of northeast China. Sci. Total Environ. 689, 312-321.

Phillips, S.M., Bellcross, A.D., Smith, G.D., 2017. Light Absorption by Brown Carbon in the Southeastern United States is pH-dependent. Environ. Sci. Technol. 51, 6782-6790.

Pillar-Little, E.A., Guzman, M.I., 2018. An Overview of Dynamic Heterogeneous Oxidations in the Troposphere. Environments 5, 104.

Qin, J., Zhang, L., Qin, Y., Shi, S., Li, J., Gao, Y., Tan, J., Wang, X., 2022. pH-Dependent Chemical Transformations of Humic-Like Substances and Further Cognitions Revealed by Optical Methods. Environ. Sci. Technol. 56, 7578-7587.

Qin, J., Zhang, L., Zhou, X., Duan, J., Mu, S., Xiao, K., Hu, J., Tan, J., 2018. Fluorescence fingerprinting properties for exploring water-soluble organic compounds in PM 2.5 in an industrial city of northwest China. Atmos. Environ. 184, 203-211.

Santos, P.S.M., Otero, M., Duarte, R.M.B.O., Duarte, A.C., 2009. Spectroscopic characterization of dissolved organic matter isolated from rainwater. Chemosphere 74, 1053-1061.

Santos, P.S.M., Santos, E.B.H., Duarte, A.C., 2012. First spectroscopic study on the structural features of dissolved organic matter isolated from rainwater in different seasons. Sci. Total Environ. 426, 172-179.

Song, J., Li, M., Jiang, B., Wei, S., Fan, X., Peng, P., 2018. Molecular Characterization of Water-Soluble Humic like Substances in Smoke Particles Emitted from Combustion of Biomass Materials and Coal Using Ultrahigh-Resolution Electrospray Ionization Fourier Transform Ion Cyclotron Resonance Mass Spectrometry. Environ. Sci. Technol. 52, 2575-2585.

Song, J., Li, M., Zou, C., Cao, T., Fan, X., Jiang, B., Yu, Z., Jia, W., Peng, P.a., 2022. Molecular Characterization of Nitrogen-Containing Compounds in Humic-like Substances Emitted from Biomass Burning and Coal Combustion. Environ. Sci. Technol. 56, 119-130.

https://doi.org/10.5194/egusphere-2023-2029
Preprint. Discussion started: 5 October 2023

Song, J.Z., Huang, W.L., Peng, P.A., Xiao, B.H., Ma, Y.J., 2010. Humic Acid Molecular Weight Estimation by High-Performance Size-Exclusion Chromatography with Ultraviolet Absorbance Detection and Refractive Index Detection. Soil. Sci. Soc. Am. J. 74, 2013-2020.

Sun, H., Li, X., Zhu, C., Huo, Y., Zhu, Z., Wei, Y., Yao, L., Xiao, H., Chen, J., 2021. Molecular composition and optical property of humic-like substances (HULIS) in winter-time PM2.5 in the rural area of North China Plain. Atmos. Environ. 252, 118316.

Sun, H., Wu, Z., Kang, X., Zhu, C., Yu, L., Li, R., Lin, Z., Chen, J., 2023. Molecular characterization of humic-like substances (HULIS) in atmospheric particles (PM2.5) in offshore Eastern China Sea (OECS) using solid-phase extraction coupled with ESI FT-ICR MS. Atmos. Environ. 294, 119523.

Tang, J., Li, J., Mo, Y., Safaei Khorram, M., Chen, Y., Tang, J., Zhang, Y., Song, J., Zhang, G., 2020. Light absorption and emissions inventory of humic-like substances from simulated rainforest biomass burning in Southeast Asia. Environmental Pollution 262, 114266.

Wang, K., Zhang, Y., Huang, R.-J., Cao, J., Hoffmann, T., 2018. UHPLC-Orbitrap mass spectrometric characterization of organic aerosol from a central European city (Mainz, Germany) and a Chinese megacity (Beijing). Atmos. Environ. 189, 22-29.

Wang, X., Qin, Y., Qin, J., Long, X., Qi, T., Chen, R., Xiao, K., Tan, J., 2021a. Spectroscopic insight into the pH-dependent interactions between atmospheric heavy metals (Cu and Zn) and water-soluble organic compounds in PM2.5. Sci. Total Environ. 767, 145261.

Wang, X.B., Qin, Y.Y., Qin, J.J., Yang, Y.R., Qi, T., Chen, R.Z., Tan, J.H., Xiao, K., 2021b. The interaction laws of atmospheric heavy metal ions and water-soluble organic compounds in PM2.5 based on the excitation-emission matrix fluorescence spectroscopy. Journal of Hazardous Materials 402, 8.

Wang, Y., Hu, M., Lin, P., Tan, T., Li, M., Xu, N., Zheng, J., Du, Z., Qin, Y., Wu, Y., Lu, S., Song, Y., Wu, Z., Guo, S., Zeng, L., Huang, X., He, L., 2019. Enhancement in Particulate Organic Nitrogen and Light Absorption of Humic-Like Substances over Tibetan Plateau Due to Long-Range Transported Biomass Burning Emissions. Environ. Sci. Technol. 53, 14222-14232.

Win, M.S., Tian, Z., Zhao, H., Xiao, K., Peng, J., Shang, Y., Wu, M., Xiu, G., Lu, S., Yonemochi, S., Wang, Q., 2018. Atmospheric HULIS and its ability to mediate the reactive oxygen species (ROS): A review. J Environ Sci (China) 71, 13-31.

Wong, J.P.S., Nenes, A., Weber, R.J., 2017. Changes in Light Absorptivity of Molecular Weight Separated Brown Carbon Due to Photolytic Aging. Environ. Sci. Technol. 51, 8414-8421.

Wong, J.P.S., Tsagkaraki, M., Tsiodra, I., Mihalopoulos, N., Violaki, K., Kanakidou, M., Sciare, J., Nenes, A., Weber, R.J., 2019. Atmospheric evolution of molecular-weight-separated brown carbon from biomass burning. Atmos. Chem. Phys. 19, 7319-7334.

Wu, G., Fu, P., Ram, K., Song, J., Chen, Q., Kawamura, K., Wan, X., Kang, S., Wang, X., Laskin, A., Cong, Z., 2021. Fluorescence characteristics of water-soluble organic carbon in atmospheric aerosol☆. Environmental Pollution 268, 115906.

Wu, G., Wan, X., Gao, S., Fu, P., Yin, Y., Li, G., Zhang, G., Kang, S., Ram, K., Cong, Z., 2018. Humic-Like Substances (HULIS) in Aerosols of Central Tibetan Plateau (Nam Co, 4730 m asl): Abundance, Light Absorption Properties, and Sources. Environ. Sci. Technol. 52, 7203-7211.

Wu, G., Wan, X., Ram, K., Li, P., Liu, B., Yin, Y., Fu, P., Loewen, M., Gao, S., Kang, S., Kawamura, K., Wang, Y., Cong, Z., 2020. Light absorption, fluorescence properties and sources of brown carbon aerosols in the Southeast Tibetan Plateau. Environmental Pollution 257, 113616.

https://doi.org/10.5194/egusphere-2023-2029
Preprint. Discussion started: 5 October 2023

Yuan, W., Huang, R.-J., Yang, L., Ni, H., Wang, T., Cao, W., Duan, J., Guo, J., Huang, H., Hoffmann, T., 2021. Concentrations, optical properties and sources of humic-like substances (HULIS) in fine particulate matter in Xi'an, Northwest China. Sci. Total Environ. 789, 147902.

Zeng, Y., Ning, Y., Shen, Z., Zhang, L., Zhang, T., Lei, Y., Zhang, Q., Li, G., Xu, H., Ho, S.S.H., Cao, J., 2021. The Roles of N, S, and O in Molecular Absorption Features of Brown Carbon in PM2.5 in a Typical Semi-Arid Megacity in Northwestern China. Journal of Geophysical Research: Atmospheres 126, e2021JD034791.

Zhang, T., Huang, S., Wang, D., Sun, J., Zhang, Q., Xu, H., Hang Ho, S.S., Cao, J., Shen, Z., 2022a. Seasonal and diurnal variation of PM2.5 HULIS over Xi'an in Northwest China: Optical properties, chemical functional group, and relationship with reactive oxygen species (ROS). Atmos. Environ. 268, 118782.

Zhang, T., Shen, Z., Huang, S., Lei, Y., Zeng, Y., Sun, J., Zhang, Q., Ho, S.S.H., Xu, H., Cao, J., 2022b. Optical properties, molecular characterizations, and oxidative potentials of different polarity levels of water-soluble organic matters in winter PM2.5 in six China's megacities. Sci. Total Environ. 853, 158600.

Zhang, T., Shen, Z., Zeng, Y., Cheng, C., Wang, D., Zhang, Q., Lei, Y., Zhang, Y., Sun, J., Xu, H., Ho, S.S.H., Cao, J., 2021. Light absorption properties and molecular profiles of HULIS in PM2.5 emitted from biomass burning in traditional “Heated Kang” in Northwest China. Sci. Total Environ. 776, 146014.

Zhang, T., Shen, Z., Zhang, L., Tang, Z., Zhang, Q., Chen, Q., Lei, Y., Zeng, Y., Xu, H., Cao, J., 2020. PM2.5 Humic-like substances over Xi'an, China: Optical properties, chemical functional group, and source identification. Atmos. Res. 234, 104784.

Zhang, W., Li, L., Wang, D., Wang, R., Yu, S., Gao, N., 2022c. Characterizing dissolved organic matter in aquatic environments by size exclusion chromatography coupled with multiple detectors. Anal. Chim. Acta 1191, 339358.

Zheng, G.J., He, K.B., Duan, F.K., Cheng, Y., Ma, Y.L., 2013. Measurement of humic-like substances in aerosols: A review. Environmental Pollution 181, 301-314.

Zou, C., Cao, T., Li, M., Song, J., Jiang, B., Jia, W., Li, J., Ding, X., Yu, Z., Zhang, G., Peng, P.a., 2023. Measurement report: Changes in light absorption and molecular composition of water-soluble humic-like substances during a winter haze bloom-decay process in Guangzhou, China. Atmos. Chem. Phys. 23, 963-979.

Zou, C., Li, M., Cao, T., Zhu, M., Fan, X., Peng, S., Song, J., Jiang, B., Jia, W., Yu, C., Song, H., Yu, Z., Li, J., Zhang, G., Peng, P.a., 2020. Comparison of solid phase extraction methods for the measurement of humic-like substances (HULIS) in atmospheric particles. Atmos. Environ. 225, 117370.